



Huang, C., Chen, R., & Ke, Q., et al. (2011). Electrospun collagen-chitosan-TPU nanofibrous scaffolds for tissue engineered tubular grafts.

Originally published in *Colloids and Surfaces B: Biointerfaces*, 82(2), 307–315.

Available from: <http://dx.doi.org/10.1016/j.colsurfb.2010.09.002>

Copyright © 2010 Elsevier BV. All rights reserved.

This is the author's version of the work. It is posted here with the permission of the publisher for your personal use. No further distribution is permitted. If your library has a subscription to this journal, you may also be able to access the published version via the library catalogue.



## Accepted Manuscript

Title: Electrospun collagen-chitosan-TPU nanofibrous scaffolds for tissue engineered tubular grafts

Authors: Chen Huang, Rui Chen, Qinfei Ke, Yosry Morsi, Kuihua Zhang, Xiumei Mo



PII: S0927-7765(10)00509-6  
DOI: doi:10.1016/j.colsurfb.2010.09.002  
Reference: COLSUB 4248

To appear in: *Colloids and Surfaces B: Biointerfaces*

Received date: 30-7-2010  
Revised date: 26-8-2010  
Accepted date: 1-9-2010

Please cite this article as: C. Huang, R. Chen, Q. Ke, Y. Morsi, K. Zhang, X. Mo, Electrospun collagen-chitosan-TPU nanofibrous scaffolds for tissue engineered tubular grafts, *Colloids and Surfaces B: Biointerfaces* (2010), doi:10.1016/j.colsurfb.2010.09.002

This is a PDF file of an unedited manuscript that has been accepted for publication. As a service to our customers we are providing this early version of the manuscript. The manuscript will undergo copyediting, typesetting, and review of the resulting proof before it is published in its final form. Please note that during the production process errors may be discovered which could affect the content, and all legal disclaimers that apply to the journal pertain.

1      **Electrospun collagen-chitosan-TPU nanofibrous scaffolds for tissue**  
2                                      **engineered tubular grafts**

3      Chen Huang<sup>1, 2</sup>, Rui Chen<sup>1, 2</sup>, Qinfei Ke<sup>1, 2</sup>, Yosry Morsi<sup>3</sup>, Kuihua Zhang<sup>1, 4</sup>, and  
4      Xiumei Mo<sup>1\*</sup>

5      1. Key Laboratory of Textile Science & Technology, Ministry of Education, Donghua University,  
6                                      Shanghai, P. R. China 201620

7                                      2. College of textiles, Donghua University, Shanghai, 201620, China

8      3. Faculty of engineering and industry science, Swinburne University of Technology, Melbourne,  
9                                      Victoria, 3122, Australia

10     4. College of Biological Engineering and Chemical Engineering, Jiaxing College, Zhejiang,  
11                                      314001, China.

12     \* Corresponding Author: Prof. Mo Xiumei Ph.D, Director of Biomaterials and Tissue Engineering,  
13                                      Donghua University, 2999 Renmin Rd. North, Songjiang District Shanghai China, 201620

14                                      Phone: 86-21-67792653, Fax: 86-21-67792653, Email: xmm@dhu.edu.cn

15     **Abstract:** The objective of this study is to design a novel kind of scaffolds for blood vessel and  
16     nerve repairs. Random and aligned nanofibrous scaffolds based on collagen-chitosan-thermoplastic  
17     polyurethane (TPU) blends were electrospun to mimic the componential and structural aspects of  
18     the native extracellular matrix, while an optimal proportion was found to keep the balance between  
19     biocompatibility and mechanical strength. The scaffolds were crosslinked by glutaraldehyde (GTA)  
20     vapor to prevent them from being dissolved in the culture medium. Fiber morphology was  
21     characterized using scanning electron microscopy (SEM) and atomic force microscopy (AFM).  
22     Fourier transform infrared spectroscopy (FTIR) showed that the three-material system exhibits no  
23     significant differences before and after crosslinking, whereas pore size of crosslinked scaffolds  
24     decreased drastically. The mechanical properties of the scaffolds were found to be flexible with a  
25     high tensile strength. Cell viability studies with endothelial cells and schwann cells demonstrated  
26     that the blended nanofibrous scaffolds formed by electrospinning process had good  
27     biocompatibility and aligned fibers could regulate cell morphology by inducing cell orientation.  
28     Vascular grafts and nerve conduits were electrospun or sutured based on the nanofibrous scaffolds

1 and the results indicated that collagen-chitosan-TPU blended nanofibrous scaffolds might be a  
2 potential candidate for vascular repair and nerve regeneration.

3 **Key words:** electrospun; collagen-chitosan-TPU; nanofibrous scaffolds; cell morphology; tissue  
4 engineering

5

Accepted Manuscript

## 1 **1. Introduction**

2 Autologous vein and artery segments have been claimed as the gold substitution for the repair of  
3 diseased vessels and peripheral nerve [1-3]. While Vascular and nerve-related diseases can occur at  
4 any age in males and females, they become increasingly common as people get older. In those cases,  
5 the use of prosthetic vascular grafts can be offered as alternatives, as suitable autologous  
6 substitutions are probably not available. Tissue engineered grafts have been proposed as a  
7 promising solution, which involves the incorporation of isolated living cells from patients into  
8 three-dimensional scaffolds, followed by the transplantation of this scaffold back into the patient  
9 via surgery.

10 As a recently developed technology, tissue engineering is a multidisciplinary subject that  
11 combines genetic engineering of cells with chemical engineering to create artificial organs and  
12 tissues, such as skin, bones, blood vessels and nerve conduits [4]. The main challenge for tissue  
13 engineered scaffolds is to design and fabricate customizable biodegradable matrices that can mimic  
14 the componential and structural aspects of extracellular matrices (ECM) [5]. Native ECM includes  
15 the interstitial matrix and the basement membrane. Gels of polysaccharides and fibrous proteins  
16 (collagen in particular) fill the interstitial space and act as a compression buffer against the stress  
17 placed on the ECM. Basement membranes are sheet-like depositions of ECM on which various  
18 epithelial cells rest [6]. Based on these facts, this study selected collagen as the protein part and  
19 chitosan as the polysaccharide part to fabricate ideal tissue engineered scaffolds.

20 As the main protein of connective tissue in animals and the most abundant protein in mammals  
21 [7], collagen is widely used as biomaterials in wound dressing and medical fields. Chitosan, a  
22 massive natural polysaccharide derived from chitin, could be used to replace glycosaminoglycan,  
23 which is the main component of natural ECM [8]. Both collagen and chitosan possess good  
24 biocompatibility, appropriate biodegradability and commercial availability. Various studies have  
25 found that collagen-chitosan complex might be an excellent candidate for tissue engineering due to  
26 its good cell viability [8-10]. However, there remains a non-ignorable gap between lab activities  
27 and clinical trials for the application of this type of complex, as the two materials are both too  
28 fragile to provide sufficient mechanical strength, which is indispensable for a successful tubular  
29 scaffold. Therefore, thermoplastic polyurethane (TPU) would be a good candidate for

1 reinforcement. As a thermal-plastic elastomer, TPU has been widely used as coating materials for  
2 breast implants, catheters, and prosthetic heart valve leaflets because of its supreme mechanical  
3 properties [11]. Although conventional TPUs are not intended to degrade, they are susceptible to  
4 hydrolytic, oxidative and enzymatic degradation in vivo.

5 In native ECM, interstitial matrix is presented as a three-dimensional structure formed by  
6 nanofibers. To architecturally mimic that structure, electrospinning technique was used because  
7 electrospun nanofiber matrices are characterized by ultrafine continuous fibers; high  
8 surface-to-volume ratio; high porosity and variable pore-size distribution, all of which are  
9 morphologically similar to the natural ECM [12]. As a simple but productive method, in recent  
10 years electrospinning technique has been widely used in biomedical fields for the production of  
11 both nonwoven and regulated matrixes [13-18].

12 Electrospinning technique provides a simple way to obtain nanofibers from both synthetic  
13 polymers and natural materials with the potential for tissue regeneration and repair.  
14 Collagen-chitosan electrospun complex and their biocompatibility have been reported previously  
15 [8, 19], however, so far the scaffolds have not been successfully applied in blood vessel and nerve  
16 repair due to the mechanical limitation of natural materials. To overcome the problem, optimal  
17 ratio of collagen/chitosan/TPU has been selected to obtain a compromise between biocompatibility  
18 and mechanical strength in the present study. Glutaraldehyde vapor (GTA) crosslinking has been  
19 conducted to prevent collagen and chitosan from being dissolved in the water. Endothelial cells and  
20 Schwann cells were then seeded on the scaffolds to examine if the three-material based scaffold  
21 could be a suitable candidate for blood vessels and nerve repair. The orientation of electrospun  
22 nanofibers plays an important role in cell growth and related functions [20-24]. Therefore, aligned  
23 nanofibrous scaffolds were prepared to regulate cell morphology in this study. SEM and  
24 Hematoxylin and eosin (H&E) staining images of cultured scaffolds demonstrated that both  
25 endothelial cells and Schwann cells have the propensity to grow along the direction of fibre  
26 alignment to some extent. Mechanical measurements of random and aligned fibrous matrices  
27 indicated that the limitation of natural materials could be solved by adding a low proportion of TPU  
28 into the mixture and such type of electrospun fibrous matrices might be a novel biomimetic tissue  
29 engineered scaffolds in vessel and nerve repair.

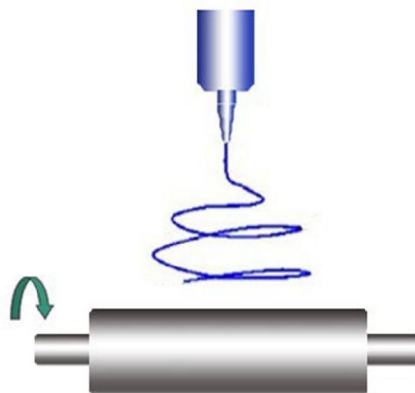
## 1 **2. Materials and methods**

### 2 **2.1. Materials**

3 Collagen I (mol. wt.,  $0.8-1 \times 10^5$  Da) was purchased from Sichuan Ming-rang Bio-Tech Co. Ltd.  
4 (China), chitosan (85%, deacetylated,  $M_n \approx 10^6$ ) was purchased from Ji-nan Haidebei Marine  
5 Bioengineering Co. Ltd. (China) and TPU polymer (Tecoflex EG-80A) was purchased from  
6 Noveon, Inc. (USA). 1,1,1,3,3,3-hexafluoroisopropanol (HFP) from Fluorochem Ltd. (UK) and  
7 trifluoroacetic acid (TFA) from Sinopharm Chemical Reagent Co., Ltd. (China) were used to  
8 dissolve the collagen, chitosan, TPU and their blends. A crosslinking agent of aqueous  
9 glutaraldehyde (GTA) solution (25%) was purchased from Sinopharm Chemical Reagent Co., Ltd.  
10 (China). Porcine iliac artery endothelial cells (PIECs) and Schwann cells (SCs) were obtained from  
11 the Institute of Biochemistry and Cell Biology (Chinese Academy of Sciences, China). All culture  
12 media and reagents were purchased from Gibco Life Technologies CO, USA unless specified.

### 13 **2.2. Electrospinning of collagen-chitosan-TPU scaffolds**

14 Collagen (8wt %) and TPU (6wt %) were dissolved in HFP while chitosan (8wt %) was dissolved  
15 in HFP/TFA mixture (v/v, 90/10). Before electrospinning, the three solutions were blended at a  
16 weight ratio of collagen/chitosan/TPU=60%/15%/25% with sufficient stirring at room temperature  
17 for 1h. The solutions were then filled into a 2.5 ml plastic syringe with a blunt-ended needle. The  
18 syringe was attached to a syringe pump (789100C, Cole-Pamer, America) and dispensed at a rate of  
19 1.0 ml/h. A voltage of 18KV was obtained from a high voltage power supply (BGG6-358,  
20 BMEICO.LTD. China) and applied across the needle and ground collector. Random nanofibers  
21 were collected on a flat collector plate wrapped with aluminum foil at a distance of 12-15cm.  
22 Aligned nanofibers were formed on a rotating drum with a 6 cm diameter, rotation speed of  
23 4000r/min and 12cm away from the tip of the syringe [Fig.1]. To compare orientation degree, pure  
24 TPU nanofibers were electrospun using the same parameters as above.



1

2

**Fig.1.** Schematic diagram of electrospinning spinneret and rotating drum

3

### **2.3. GTA vapor crosslinking**

4

The crosslinking process was carried out by placing the collagen-chitosan-TPU nanofibrous

5

membrane in a sealed, dual-layered desiccator containing 10 ml of 25% glutaraldehyde aqueous

6

solution in a Petri dish. The membranes were fixed on a glass frame and were crosslinked in an

7

atmosphere of water and glutaraldehyde vapor at room temperature for 2 days. The Petri dish was

8

placed inside the bottom layer of the desiccator, whilst the nanofibrous membrane was fixed on a

9

glass frame in the upper layer, above the semi-permeable divider. After crosslinking, samples were

10

exposed in the vacuum oven at normal room temperature.

11

### **2.4. Characterization**

12

Fiber morphology was observed with a scanning electronic microscope (SEM) (JSM-5600, Japan)

13

at an accelerated voltage of 10KV. The fibers were coated with gold sputter. Fiber diameters were

14

estimated using image analysis software (Image-J, National Institutes of Health, USA) and

15

calculated by selecting 100 fibers randomly observed on the SEM images. A two-dimensional fast

16

Fourier transform (2D FFT) approach [25] was adapted to measure fiber alignment in electrospun

17

matrix. Surface properties of the nanofibers were examined using a nanoscope atomic-force

18

microscope (Nanoscope IV, America), in the tapping mode and expressed as height and phase

19

images.



1 Fourier transform infrared spectroscopy (FTIR) studies were carried out on compressed films  
2 containing KBr pellets and samples using a FTIR spectrophotometer (Avatar380, USA). All  
3 spectra were recorded in absorption mode at  $2\text{cm}^{-1}$  interval and in the wavelength range 4000–600  
4  $\text{cm}^{-1}$ .

5 The tensile strength test was performed on various electrospun collagen-chitosan-TPU specimens  
6 ( $n=6$  for each group) with random, parallel or perpendicular fiber alignment. All samples were of  
7 same size (30 x 10mm), and the test was performed using a universal materials tester (H5 K-S,  
8 Hounsfield, UK) with a 50 N load cell at ambient temperature of  $20^\circ\text{C}$  and humidity of 65%. A  
9 cross-head speed of 10 mm/min was used for all the specimens tested.

10 Electrospun nanofibrous scaffolds were cut into  $30\times 30$  mm squares for porometry measurement.  
11 A CFP-1100-AI capillary flow porometer (PMI Porous Materials Int.) was used in this study to  
12 measure pore size and pore distribution. Calwick with a surface tension of 21 dynes/cm (PMI  
13 Porous Materials Int.) was used as the wetting agent for porometry measurements. For each group,  
14 the test was repeated 3 times to gain a better accuracy.

## 15 **2.5. Viability and morphology studies of PIECs and SCs**

16 Porcine iliac artery endothelial cells and Schwann cells were cultured respectively in Dulbecco's  
17 modified Eagle's medium (DMEM) and DMEM/F12 1:1 mixture medium with 10% fetal bovine  
18 serum and 1% antibiotic-antimycotic at an atmosphere of 5%  $\text{CO}_2$  and  $37^\circ\text{C}$ . The medium was  
19 replenished every three days. Electrospun scaffolds were prepared on circular glass coverslips  
20 (14mm in diameter), which were then placed into the wells on a 24-well plate individually, and  
21 being secured with stainless rings. Before seeding cells, scaffolds were sterilized by immersion in  
22 75% ethanol for 2 hours, washed 3 times with phosphate-buffered saline solution (PBS), and then  
23 washed with culture medium. Cells were then seeded at a density of  $1.0\times 10^4$  cells/well of 24-well  
24 plates and tissue culture polystyrene (TCP) wells were seeded as control.

25 Cell viability on electrospun scaffolds was determined by methylthiazol tetrazolium (MTT) assay  
26 ( $n=6$  for each assay). After 1, 3, 5 and 7 days of cell seeding, the cells and matrices were incubated  
27 with 5mg/ml 3-[4, 5-dimethyl-2-thiazolyl]-2, 5-diphenyl-2H-tetrazolium bromide (MTT) for 4h.  
28 Thereafter, the culture media were extracted and 400uL MTT were added for about 20 min. When  
29 the crystal was sufficiently dissolved, aliquots were pipetted into the wells of a 96-well plate and

1 tested by an Enzyme-labeled Instrument (MK3, Thermo, USA), and the UV absorbance at 490nm  
2 for each well was measured.

3 Cell morphology was examined by SEM after 3 days of culturing. The scaffolds were rinsed  
4 twice with PBS and fixed in 4% glutaraldehyde aqueous solution at 4°C for 2h. Fixed samples were  
5 rinsed twice with PBS and then dehydrated in gradient concentrations of ethanol (30, 50, 70, 80, 90,  
6 95 and 100%). After being dried in vacuum oven overnight, the cellular constructs were coated  
7 with gold sputter and observed under the SEM at a voltage of 10KV. Hematoxylin and eosin (H&E)  
8 staining was also conducted on thinner scaffolds (thickness  $\leq 100 \mu\text{m}$ ) as complements to observe  
9 cell morphology.

### 10 **3. Results and discussion**

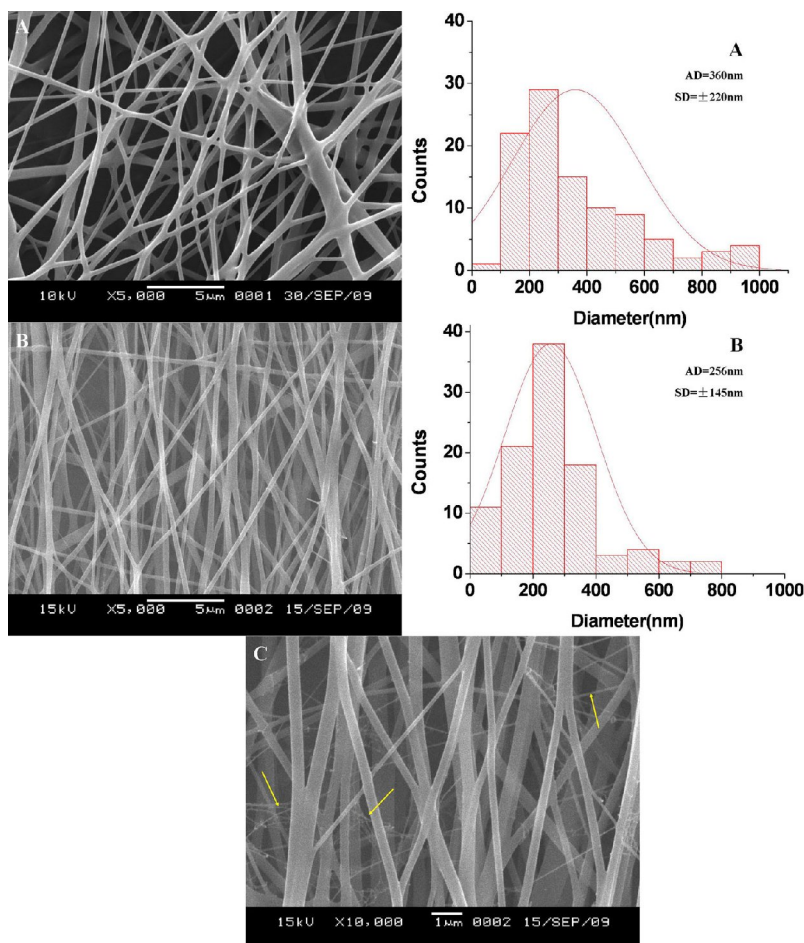
#### 11 **3.1. Morphology of electrospun fibers**

12 It is generally accepted that nanofiber diameter, surface morphology and pore-size distribution  
13 could be affected apparently by electrospinning parameters including needle size, working distance,  
14 applied voltage, flow rate and working environment. To investigate the morphology of electrospun  
15 fibers, SEM micrographs of randomly oriented and aligned collagen-chitosan-TPU nanofibrous  
16 scaffolds were acquired with fiber diameter in the range of  $360\pm 220$  and  $256\pm 145$  nm, respectively  
17 (Fig.2A and Fig.2B). The reason why aligned nanofibers has a comparatively lower average  
18 diameter than that of randomly oriented nanofibers is probably because with such a high rotating  
19 speed, fibers are stretched and thus attenuated as soon as they reached the rotating collector. When  
20 the scaffolds were amplified to magnification $\times 10000$ , many superfine fibers (diameter  $\leq 100\text{nm}$ )  
21 can be observed from Fig.2C (pointed by the arrows) and the existence of these fibers could be  
22 explained by the positive charges carried by chitosan, which makes the mixture solution a more  
23 complicated system. These increased charges would increase solution conductivity and since the  
24 force that causes the stretching of the solution could be ascribed to the repulsive forces between the  
25 charges on the electrospinning jet, the stretching process would be enhanced owing to the increase  
26 of solution conductivity.

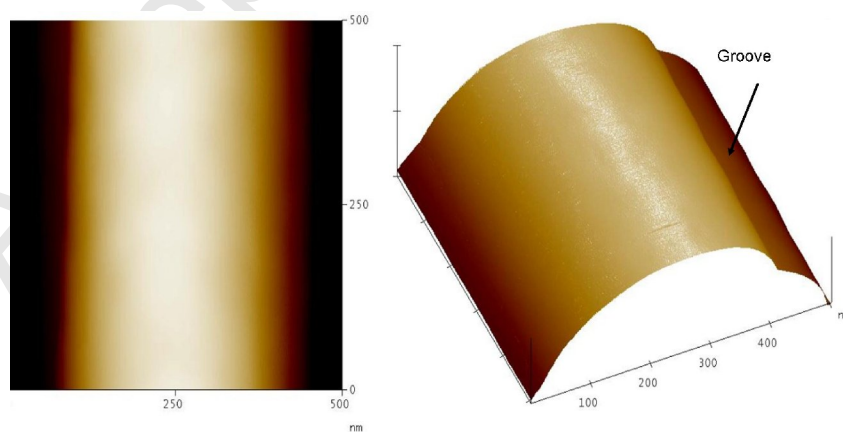
27 To observe the surface morphologies of collagen-chitosan-TPU nanofibers, atomic-force  
28 microscopy (AFM) was employed by using height mode (Fig.3). It was reported that the surface of  
29 electrospun collagen fibers was comparatively rougher than that of electrospun synthetic

1 polymers[26], whereas from our AFM images, with a TPU proportion of 25% it could be clearly  
2 observed that the surface of collagen-chitosan-TPU nanofibers was quite smooth and a groove on  
3 the right side of the fiber could be found. This phenomenon might be attributed to the complexity of  
4 mixture solution while the grooves were not found on all the fibers. From surface morphology  
5 images we can see that TPU component could improve the spinnability of polymer solution while  
6 the existence of grooves on some nanofibers would be conducive to cell adhesion and proliferation  
7 by providing adhesion sites for cell growth.

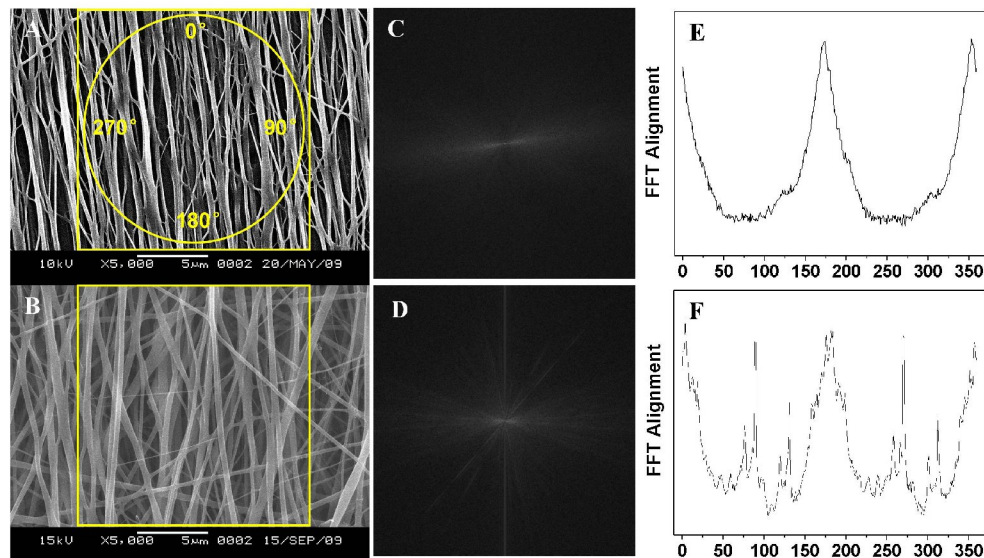
8 With the aim of measuring fiber alignment, a two-dimensional fast Fourier transform (2D FFT)  
9 approach described by Ayres et al [25] was adapted. In brief, a quadrature region was captured from  
10 SEM images (Fig.4A and Fig.4B) and then analyzed with ImageJ software to create corresponding  
11 frequency plots and 2D FFT alignment plots. The two peaks at  $175^\circ$  and  $355^\circ$  in Fig.4E show that  
12 with a rotation speed of 4000r/min, pure TPU nanofibers were highly arrayed along one direction,  
13 however, in the three-material based system (Fig.4F), fiber orientation could not be regulated with  
14 such a high uniformity. Although two main peaks could also be found at  $5^\circ$  and  $185^\circ$ , the existence  
15 of other peaks indicates that some nanofibers are not well aligned. This phenomenon demonstrates  
16 that besides ambient parameters such as applied voltage and rotating speed, properties of mixture  
17 solution (difference in molecular weight and electric-charge number) also play an indispensable  
18 role in the determination of fiber morphology.



1  
2 **Fig.2.** SEM micrographs of collagen-chitosan-TPU nanofibers and their diameter distribution: (A)  
3 random oriented nanofibers; (B), (C) aligned nanofibers with 5000 and 10000 magnification.  
4



5  
6 **Fig.3.** AFM images represented by height model

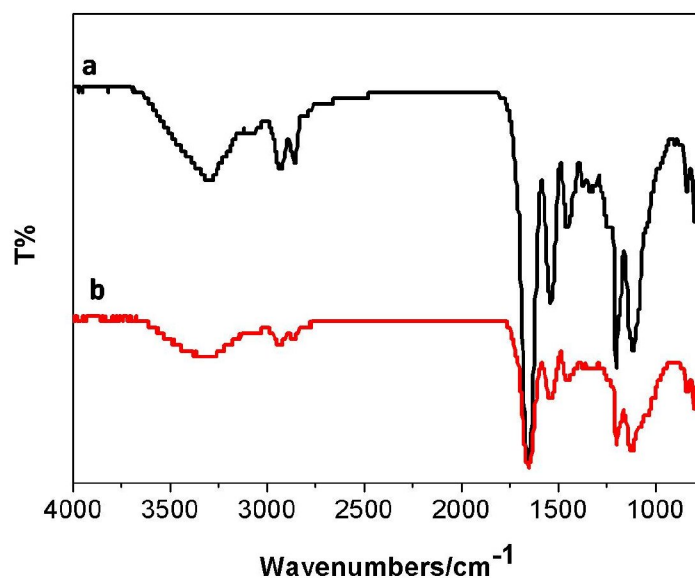


1  
2 **Fig.4.** SEM images of aligned electrospun scaffolds with a rotation speed of 4000r/min (A  
3 represents pure TPU nanofibers while B represents collagen-chitosan-TPU nanofibers). ImageJ  
4 frequency plots (C, D) and 2D FFT alignment plots (E, F) for the corresponding quadrature regions.

### 5 **3.2. Fourier Transform Infrared Spectroscopy**

6 In a complicated system containing three types of materials, the Fourier transform infrared  
7 spectroscopy (FTIR) could be used as an effective method to define the existence of each  
8 component. FTIR spectra of electrospun collagen–chitosan and collagen-TPU nanofibers were  
9 studied in previous work [8, 26]. Fig.5 depicted the FTIR spectra of non-crosslinked (Fig.5a) and  
10 crosslinked (Fig.5b) collagen-chitosan-TPU fibers with a weight ratio of 60%:15%:25% (collagen:  
11 chitosan: TPU).

12 As shown in Fig.5a, the characteristic absorption bands of collagen were observed at  
13  $1650\text{cm}^{-1}$  (amide I),  $1530\text{cm}^{-1}$  (amide II),  $1200\text{cm}^{-1}$  (amide III) respectively while the peak at  $1130$   
14  $\text{cm}^{-1}$  was assigned to chitosan for its saccharine structure. N-H and C-H stretches at  $2940\text{cm}^{-1}$  and  
15  $3300\text{cm}^{-1}$  and other peaks overlapped with collagen between  $1530\text{cm}^{-1}$  to  $1200\text{cm}^{-1}$  were  
16 characteristic of TPU. Compared to Fig.5a, Fig.5b showed no significant difference in the location  
17 of these characteristic peaks, this is probably because the absorption peak of  $\text{—C=N—}$  stretching  
18 vibration generated by GTA crosslinking could be in the range of  $1640\text{cm}^{-1}$  to  $1690\text{cm}^{-1}$  and an  
19 overlap might've occurred with the strong absorption of the amide I band.



1  
2 **Fig.5.** FTIR spectra of coaxial collagen-chitosan-TPU electrospun nanofibrous membranes.

3 Non-crosslinked(a); Crosslinked (b).

### 4 **3.3. Pore size**

5 For tissue engineered scaffolds, microscale and nanoscale porous structure are most favorable  
6 because the highly porous network of interconnected pores helps to facilitate the passage of  
7 nutrients and the exchange of gases, which are crucial for cellular growth and tissue regeneration  
8 [13]. Pore size and pore distribution analyses were conducted by automated capillary flow  
9 porometer system software and the results were shown in Tab.1. It could be seen that when  
10 scaffolds were similar in thickness, the mean, largest and smallest pore diameter of randomly  
11 oriented collagen-chitosan-TPU nanofibrous scaffold were all larger than the corresponding  
12 measurements of aligned. This implies that parallel alignment can decrease pore size and lead a  
13 more evenly pore size distribution. What's more, we can conclude that after GTA vapor  
14 crosslinking, nanofibrous scaffolds become more compact because specimen thickness and pore  
15 size of both random and aligned scaffolds decreased dramatically.

16  
17  
18

					Smallest pore Diameter( $\mu\text{m}$ )
					0.1796
					0.0823

1 **Tab.1.** Pore diameter of random oriented and aligned collagen-chitosan-TPU nanofibrous scaffolds

### 2 **3.4. Mechanical properties analysis**

3 In the fabrication of tubular scaffolds, mechanical strength is of vital importance to provide  
 4 enough support and this is the reason why natural materials, such as collagen and chitosan could  
 5 not be used as the dominant component for electrospun grafts. It is reported that the tensile strength  
 6 of a native artery is about 1.5Mpa [1], however, for scaffolds made from natural materials, a much  
 7 higher strength is necessary when aspects like degradation and wet-strength loss are taken into  
 8 consideration.

9 The typical tensile stress-strain curves of random oriented and aligned collagen-chitosan-TPU  
 10 nanofibrous scaffolds (non-crosslinked, crosslinked) were shown in Fig.6 while the average  
 11 elongation at break and average tensile strength of each specimen were summarized in Tab.2.  
 12 Comparing Fig.6A, B, C with Fig.6A', B', C', it can be seen that GTA vapor crosslinking had a  
 13 positive influence on tensile strength but a negative influence on average elongation at break. After  
 14 crosslinking both randomly oriented and aligned scaffolds were tended to be more stiff and brittle.  
 15 To improve elasticity of scaffold, TPU was added to natural fibers, such as collagen and chitosan.  
 16 TPU proportion of 10%, 20%, 25% and 30%. were investigated to determine the optimal  
 17 component ratio. According to our observation, blended fibrous scaffolds with TPU proportion  
 18 lower than 20% would be easily broken when squeezed or stretched, making them too fragile for  
 19 tubular applications. Therefore, TPU proportion should not be set below 25% otherwise the

1 elongation at break of crosslinked scaffolds could not exceed 10% and the scaffolds were too  
2 fragile to meet the flexibility requirements of tubular grafts.

3 The tensile strength of the aligned nanofiberous scaffolds showed significant differences between  
4 parallel ( $14.93 \pm 0.59$  MPa) and perpendicular ( $5.04 \pm 0.95$  MPa) directions. Moreover, comparison of  
5 elongation at break between scaffolds of parallel and perpendicular alignment showed an even  
6 sharper difference ( $58.92 \pm 15.46\%$  as opposed to  $8.20 \pm 0.84\%$ ).

7 As described before, GTA crosslinking had a negative affect on elongation at break, whereas at  
8 parallel direction crosslinked scaffolds boasted better elasticity than non-crosslinked ones. While  
9 aligned samples (crosslinked) were stretched along the direction of fiber orientation, there exists a  
10 unique fracture behavior. Fig.7 shows that both random and aligned samples started to rupture with  
11 a small crack when tensile strength reached peak value, however, instead of extending to  
12 neighbouring fibers, the cracks on parallel samples preferred to move along the direction of fiber  
13 orientation and a small part of the sample was torn before the breakage of the entire sample. Thus,  
14 the sample had a higher percentage reading for elongation at break, and could be stretched further.  
15 This fracture behavior could also be reflected from Fig. 6B', where a yielding point was formed on  
16 every stress-strain curve. The underlying mechanism was that unlike conventional fractures, when  
17 aligned fibers were stretched along parallel direction and formed a small crack, 'slippage' occurred  
18 amongst fibers; the paralleled fibers tended to slit along fiber orientation direction, and fractures  
19 were reduced as a result. Similar phenomenon did not occur on non-crosslinked samples, indicating  
20 that prior to GTA vapor crosslinking, scaffolds were quite sticky with a much larger sliding friction  
21 force between neighboring fibers. Therefore, the crosslinked collagen-chitosan-TPU aligned  
22 nanofibrous scaffolds, which possessed good mechanical properties at parallel direction, were more  
23 suitable for the fabrication of tissue-engineered nerve conduits.

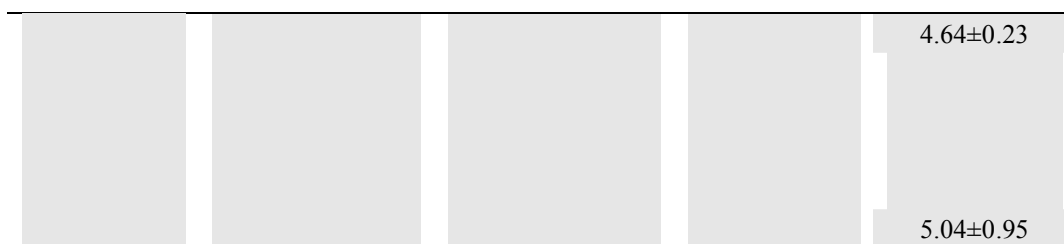
24

25

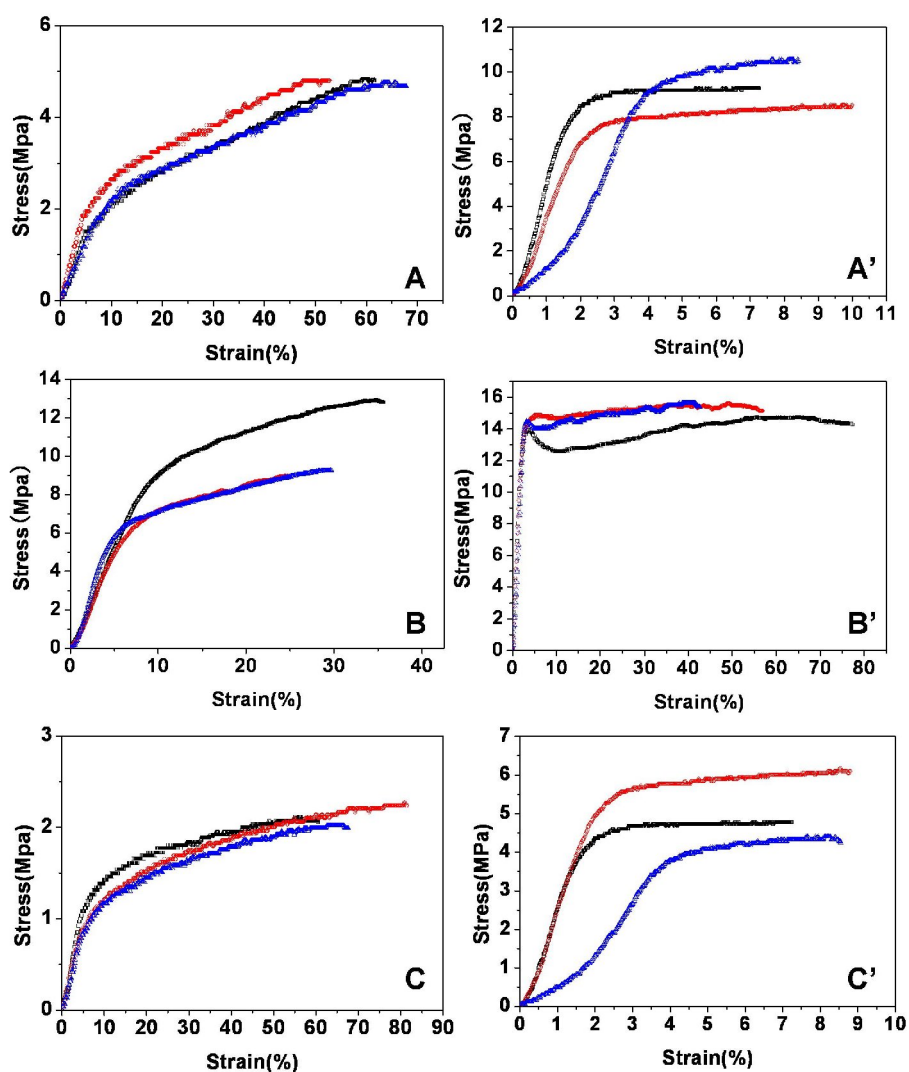
26

			Average tensile strength(MPa)



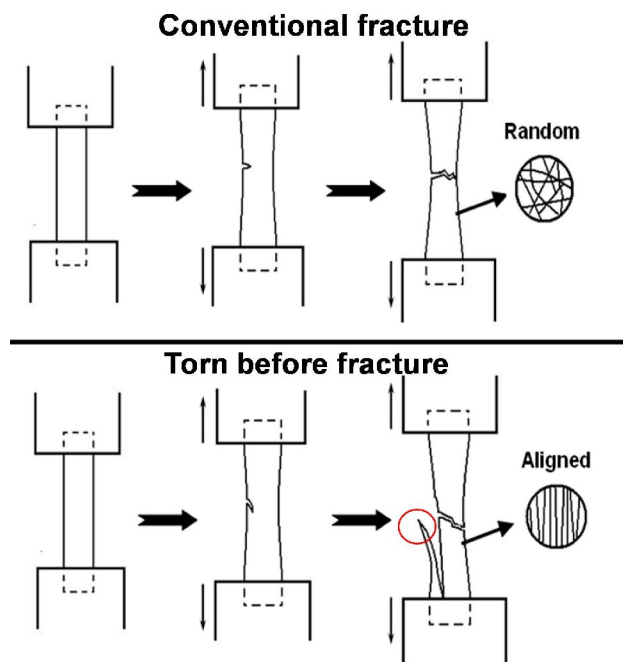


1 **Tab.2.** Mechanical properties of randomly oriented and aligned collagen-chitosan-TPU  
 2 nanofibrous scaffolds before and after GTA crosslinking. Data are representatives of 6 independent  
 3 experiments and all the data are used as means $\pm$ SD.



4  
 5 **Fig.6.** Stress-strain curves of collagen-chitosan-TPU scaffolds. (A), (A') randomly oriented  
 6 nanofibrous scaffolds before and after crosslinking; (B), (B') aligned nanofibrous scaffolds at  
 7 parallel direction before and after crosslinking; (C), (C') aligned nanofibrous scaffolds at

1 perpendicular direction before and after crosslinking.



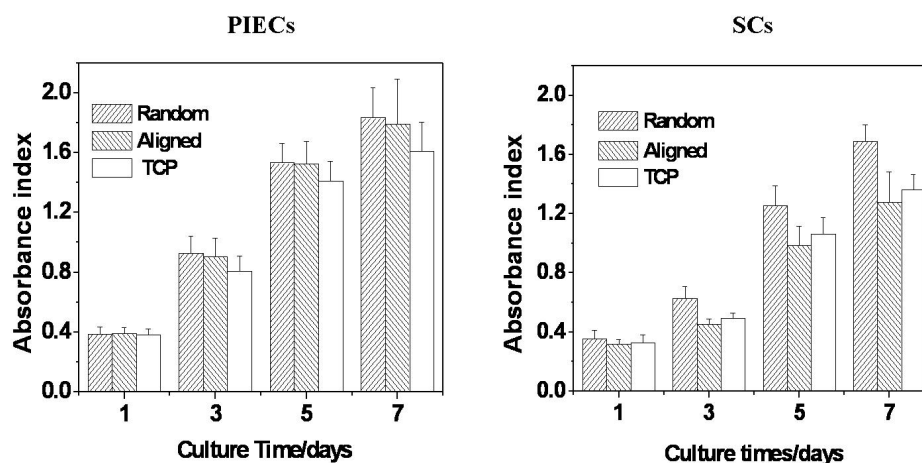
2

3 **Fig.7.** Illustration of conventional fracture and slippage along parallel direction

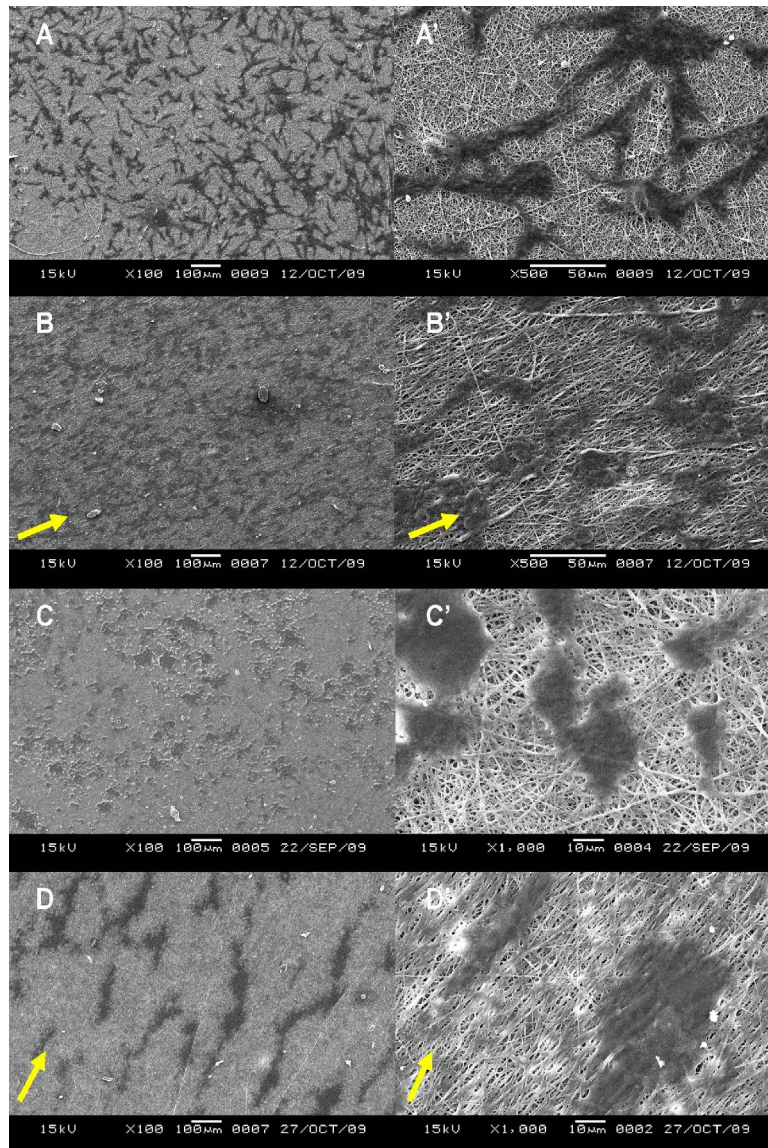
#### 4 **3.5. Viability of PIECs and SCs on nanofibrous scaffolds**

5 For tissue engineered scaffolds, surface chemistry and topography are major factors in regulating  
 6 cell behavior, including cell adhesion, cell proliferation, cell differentiation and cell morphology  
 7 [27]. Proliferation of PIECs and SCs cultured on different electrospun scaffolds was determined by  
 8 MTT assay after culturing for 1 3, 5, and 7 day and the results are shown in Fig 8. For the  
 9 proliferation of PIECs, both randomly oriented and aligned electrospun scaffolds had better cell  
 10 viability in comparison with TCP. Meanwhile, the proliferation rate of randomly oriented and  
 11 aligned scaffolds showed no significant difference, indicating that the viability of PIECs was not  
 12 affected by fiber orientation and pore size. As for SCs, random nanofibers showed a cell  
 13 proliferation of approximately 25% higher than that of aligned fibers from day 3 to day 7. It is  
 14 possible that compared with SCs, PIECs grow faster regardless of the substrate morphology, and  
 15 SCs seem to be more sensitive to the environment, which is to say that if surface morphology of the  
 16 growing media is altered, SCs viability can be easily influenced with a preference to random  
 17 fibrous scaffolds. In nerve repair, this shortage might be solved by allowing for longer culturing  
 18 duration for SCs.

1 Cell morphology and its relation with randomly oriented and aligned electrospun scaffolds were  
 2 studied in vitro for 3 days. The resulting SEM images were listed in Fig.9 and H&E staining  
 3 micrographs were listed in Fig.10 as complements. PIECs showed normal cell morphology on  
 4 random fibers (Fig.9A, 10A) whereas on aligned fibers, they seemed to show a slightly oriented  
 5 arrangement. We can see from Fig.9A' that single PIEC was still able to retain its typical cell  
 6 morphology while the orientation degree was comparatively lower. Compared to PIECs, SCs are  
 7 more responsive to the seeding matrix. As can be seen from Fig.9C and D, cells on random oriented  
 8 nanofibrous scaffolds were mostly round whereas they exhibited spindle-shaped morphology on  
 9 aligned fibers. Similar phenomenon could also be found on the H&E staining images (Fig.10 B and  
 10 B'). Unfortunately, although cell morphology could be directly identified on the H&E staining  
 11 pictures, fiber profiles are not clear. This is because once stained, colors on the protein collagen are  
 12 very difficult to be thoroughly washed away. However, it is clear from the SEM pictures that fibers  
 13 morphology and diameter were not obviously influenced by GTA crosslinking, indicating that a  
 14 GTA crosslinking period of 48h could ensure the electrospun fibers to maintain their original  
 15 morphologies in culture medium.



16  
 17 **Fig.8.** Comparison of PIEC and SC proliferation on randomly oriented and aligned  
 18 collagen-chitosan-TPU nanofibrous scaffolds and TCP.

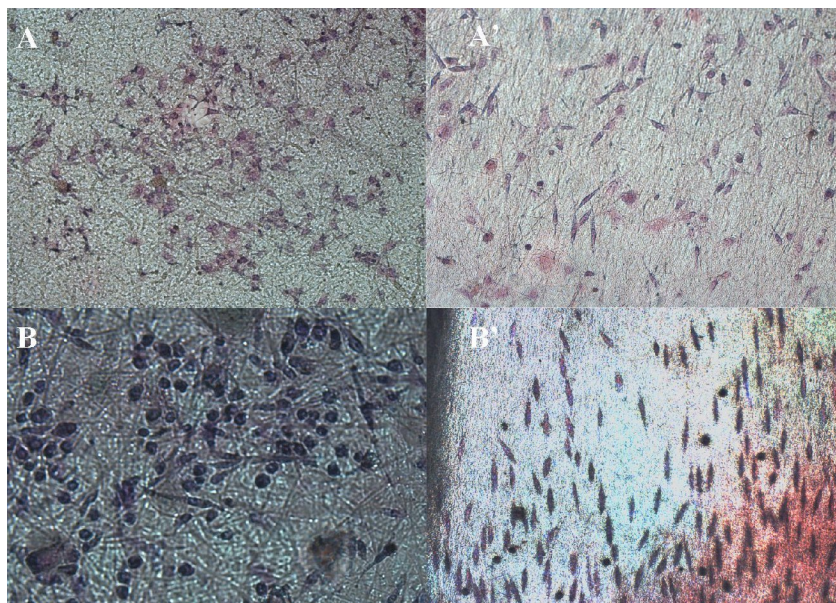


1

2 **Fig.9.** SEM micrographs of PIECs and SCs on nanofibrous scaffolds after day 3 of cell culture: (A),

3 (A') PIECs on randomly oriented nanofibers; (B), (B') PIECs on aligned nanofibers; (C), (C') SCs

4 on randomly oriented nanofibers; (D), (D') SCs on aligned nanofibers.

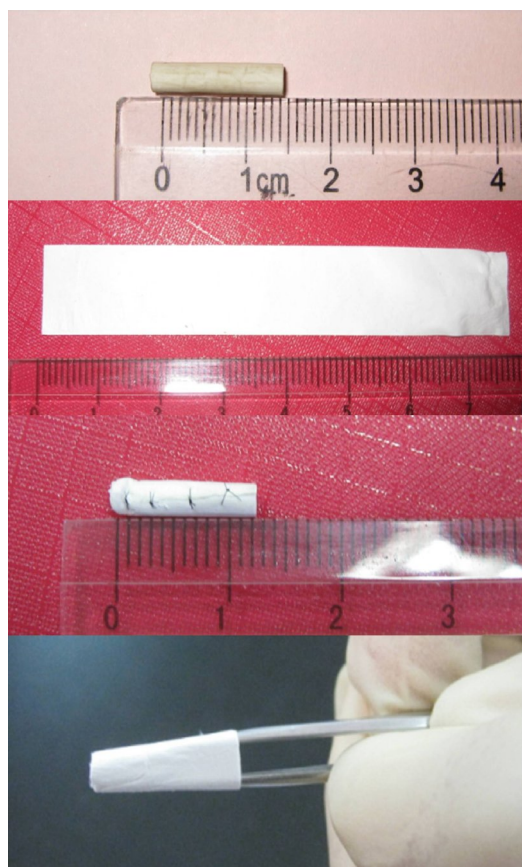


1  
2 **Fig.10.** H&E staining images of PIECs and SCs on nanofibrous scaffolds after day 3 of cell culture:  
3 (A) PIECs on randomly oriented nanofibers; (A') PIECs on aligned nanofibers; (B) SCs on  
4 randomly oriented nanofibers; (B') SCs on aligned nanofibers.

### 5 **3.6. Preparation of tubular scaffolds**

6 The aim of this study is to design a novel kind of scaffolds for blood vessel and nerve repairs, so  
7 it is necessary to find a balance between biocompatibility and mechanical strength. As is described  
8 above, collagen and chitosan were electrospun to mimic the protein-polysaccharide based structure  
9 of native ECM while the addition of TPU could support the scaffolds with enough flexibility.

10 Randomly oriented nanofibrous vascular grafts were obtained by directly electrospinning the  
11 fibers on a 3mm diameter steel cudgel with a low rotating speed (250-500 r/min). To make nerve  
12 conduits with aligned fibers, the membranes were cut into strips with fixed-size and then sutured  
13 into tubular shapes with a diameter of 1 mm. All the relevant pictures were shown in Fig. 11. From  
14 the bottom picture of Fig.11 we can see that the tubular grafts made of collagen-chitosan-TPU  
15 nanofibers have good flexibility, which guaranteed the application of these grafts in vascular repair  
16 and nerve regeneration. However, as one major purpose of electrospinning is to create seamless  
17 structures, the suturing method used in this study seems to be an imperfect method. Therefore, the  
18 method to fabricate seamless electrospun aligned fibrous tubes should be explored.



1  
2 **Fig.11.** Macrographic image of small diameter electrospun vascular graft and nerve conduit.

3  
4 **4. Conclusion**

5 In this study, a balance between biocompatibility and mechanical properties was found by  
6 adjusting the proportion of natural and synthetic materials with the aim to produce a novel type of  
7 nanofibrous scaffolds that is suitable for blood vessel and nerve repairs. Collagen and chitosan  
8 were selected to biomimic the native ECM while TPU was added to improve mechanical properties  
9 of the scaffold. Scaffold characterization and cell viability study demonstrated that the  
10 three-material based scaffolds had a profound application potential in blood vessel repair and nerve  
11 regeneration. The next step will be focused on the in vivo study of these electrospun vascular grafts  
12 and nerve conduits.

13 **Acknowledgements**

14 This research was supported by National high technology research and developed program (863

1 Program, 2008AA03Z305), “111 Project” Biomedical textile materials science and technology  
2 (B07024-SP0912) and Shanghai Unilever Research and Development Fund (08520750100).

### 3 **References**

- 4 [1] B.W. Tillman, et al., The in vivo stability of electrospun polycaprolactone-collagen scaffolds in  
5 vascular reconstruction. *Biomaterials* 30 (4) (2009) 583-588.
- 6 [2] S. Wang, et al., Acceleration effect of basic fibroblast growth factor on the regeneration of  
7 peripheral nerve through a 15-mm gap. *Journal of Biomedical Materials Research - Part A* 66  
8 (3) (2003) 522-531.
- 9 [3] P.C. Francel, et al., Regeneration of rat sciatic nerve across a LactoSorb bioresorbable conduit  
10 with interposed short-segment nerve grafts. *Journal of Neurosurgery* 99 (3) (2003) 549-554.
- 11 [4] X. Wang, P. Lin, Q. Yao, C. Chen, Development of small-diameter vascular grafts. *World*  
12 *Journal of Surgery* 31 (4) (2007) 682-689.
- 13 [5] R. Langer, J.P. Vacanti, Tissue engineering. *Science* 260 (5110) (1993) 920-926.
- 14 [6] B. Alberts, et al., *Essential cell biology*. 2004: New York and London: Garland Science.
- 15 [7] G.A. Di Lullo, et al., Mapping the ligand-binding sites and disease-associated mutations on the  
16 most abundant protein in the human, type I collagen. *Journal of Biological Chemistry* 277 (6)  
17 (2002) 4223-4231.
- 18 [8] Z.G. Chen, et al., Electrospun collagen-chitosan nanofiber: A biomimetic extracellular matrix  
19 for endothelial cell and smooth muscle cell. *Acta Biomaterialia* 6 (2) (2010) 372-382.
- 20 [9] R. Chen, et al., Preparation and characterization of coaxial electrospun thermoplastic  
21 polyurethane/collagen compound nanofibers for tissue engineering applications. *Colloids and*  
22 *Surfaces B: Biointerfaces* 79 (2) (2010) 315-325.
- 23 [10] A. Sionkowska, et al., Molecular interactions in collagen and chitosan blends. *Biomaterials* 25  
24 (5) (2004) 795-801.
- 25 [11] A. Pedicini, R.J. Farris, Mechanical behavior of electrospun polyurethane. *Polymer* 44 (22)  
26 (2003) 6857-6862.
- 27 [12] S.H. Lim, H.Q. Mao, Electrospun scaffolds for stem cell engineering. *Advanced Drug Delivery*  
28 *Reviews* 61 (12) (2009) 1084-1096.
- 29 [13] R. Murugan, S. Ramakrishna, Nano-featured scaffolds for tissue engineering: A review of  
30 spinning methodologies. *Tissue Engineering* 12 (3) (2006) 435-447.
- 31 [14] W.J. Li, et al., Electrospun nanofibrous structure: A novel scaffold for tissue engineering.  
32 *Journal of Biomedical Materials Research* 60 (4) (2002) 613-621.
- 33 [15] Z.M. Huang, Y.Z. Zhang, M. Kotaki, S. Ramakrishna, A review on polymer nanofibers by  
34 electrospinning and their applications in nanocomposites. *Composites Science and Technology*  
35 63 (15) (2003) 2223-2253.
- 36 [16] T. Courtney, et al., Design and analysis of tissue engineering scaffolds that mimic soft tissue  
37 mechanical anisotropy. *Biomaterials* 27 (19) (2006) 3631-3638.
- 38 [17] C.A. Bashur, L.A. Dahlgren, A.S. Goldstein, Effect of fiber diameter and orientation on  
39 fibroblast morphology and proliferation on electrospun poly(d,l-lactic-co-glycolic acid)  
40 meshes. *Biomaterials* 27 (33) (2006) 5681-5688.
- 41 [18] M.V. Jose, et al., Aligned PLGA/HA nanofibrous nanocomposite scaffolds for bone tissue

- 1 engineering. *Acta Biomaterialia* 5 (1) (2009) 305-315.
- 2 [19] Z. Chen, X. Mo, F. Qing, Electrospinning of collagen-chitosan complex. *Materials Letters* 61  
3 (16) (2007) 3490-3494.
- 4 [20] Z.M. Huang, et al., Fabrication of a new composite orthodontic archwire and validation by a  
5 bridging micromechanics model. *Biomaterials* 24 (17) (2003) 2941-2953.
- 6 [21] S.Y. Chew, R. Mi, A. Hoke, K.W. Leong, Aligned protein-polymer composite fibers enhance  
7 nerve regeneration: A potential tissue-engineering platform. *Advanced Functional Materials* 17  
8 (8) (2007) 1288-1296.
- 9 [22] H.B. Wang, et al., Creation of highly aligned electrospun poly-L-lactic acid fibers for nerve  
10 regeneration applications. *Journal of Neural Engineering* 6 (1) (2009).
- 11 [23] E. Schnell, et al., Guidance of glial cell migration and axonal growth on electrospun nanofibers  
12 of poly- $\epsilon$ -caprolactone and a collagen/poly- $\epsilon$ -caprolactone blend. *Biomaterials* 28 (19) (2007)  
13 3012-3025.
- 14 [24] C.H. Lee, et al., Nanofiber alignment and direction of mechanical strain affect the ECM  
15 production of human ACL fibroblast. *Biomaterials* 26 (11) (2005) 1261-1270.
- 16 [25] C.E. Ayres, et al., Measuring fiber alignment in electrospun scaffolds: A user's guide to the 2D  
17 fast Fourier transform approach. *Journal of Biomaterials Science, Polymer Edition* 19 (5) (2008)  
18 603-621.
- 19 [26] D.I. Zeugolis, et al., Electro-spinning of pure collagen nano-fibres - Just an expensive way to  
20 make gelatin? *Biomaterials* 29 (15) (2008) 2293-2305.
- 21 [27] M.M. Stevens, J.H. George, Exploring and engineering the cell surface interface. *Science* 310  
22 (5751) (2005) 1135-1138.
- 23  
24